Annals of Pure and Applied Mathematics
Vol. 3, No. 1, 2013, 17-26
ISSN: 2279-087X (P), 2279-0888(online)
Published on 16 May 2013
www.researchmathsci.org

Annals of
Pure and Applied Mathematics

Ekman Boundary Layer Mixed Convective Heat Transfer Flow through a Porous Medium with Large Suction

M. M. Haque [1]**,** ***M. S. Uddin*** [1]**,** ***M. A. Islam*** [2] **and** ***M. H. Uddin*** [3]

[1]Mathematics Discipline, Khulna University,
Khulna-9208, Bangladesh. E-mail: mm.haque@ymail.com

[2]Department of Mathematics, Damkura Hat College, Damkura,
Rajshahi, Bangladesh

[3]Department of Computer Science and Engineering,
Jessore Science & Technology University, Jessore, Bangladesh

Received 22 April 2013; accepted 26 April 2013

Abstract. An analytical investigation on a mixed convective heat transfer steady flow past a continuously moving semi-infinite vertical plate bounded by a porous medium with large suction is performed in a rotating system. The governing equations of the problem are transformed by usual similarity transformations. To solve the momentum and energy equations, the perturbation technique is used in this work. The shear stresses and Nusselt number are also calculated here. The obtained numerical values of velocities and temperature are plotted in figures. To observe the effects of various parameters on the above mentioned quantities, the results are discussed in detailed with the help of graphs as well as the tabulated values. Finally, a important conclusion is listed here.

Keywords: Ekman Boundary Layer, Mixed Convective, Heat Transfer, Suction

AMS Mathematics Subject Classification (2010): 58D30, 35Q35

1. Introduction

The flow through a porous medium plays a decisive role in many industrial applications. Porous media are very widely used to insulate a heated body to maintain its temperature. To make the heat insulation of the surface more effective, it is necessary to study the free convection flow through a porous medium. Raptis et. al. [1] have observed the steady free convective flow through a porous medium bounded by an infinite surface by use of the model of Yamamoto and Iwamura [2] for the flow near the surface. Threedimensional free convective heat transfer flow through a porous medium has been studied by Chaudhury and Chand [3].

Greenspan [4] was the first author to recognize the Ekman layer situation and he observed that, in a rotating fluid near a flat plate an Ekman layer exists wherein the viscous and Coriolis forces are of the same order of magnitude. The steady and unsteady Ekman layers of an incompressible fluid have investigated as a basic boundary layers in a rotating fluid appearing in the oceanic, atmospheric, cosmic fluid dynamics and solar physics or geophysical problems. The Ekman layer flow on a horizontal plate has been studied by Batchelor [5]. Mazumder et. al. [6] have studied the flow and heat transfer in a hydro-magnetic Ekman layer on a porous plate with Hall effects. In a rotating system, a hydromagnetic free convective flow past an impulsively started vertical plate has been observed by Singh [7].

All the above problems are investigated for free convective flow of a fluid. However, the flow by mixed convection plays a special role in a number of industrial applications such as fiber and granular insulation, geothermal systems etc. Hence, our main aim is to investigate the Ekman boundary layer mixed convective heat transfer steady flow past a continuously moving semi-infinite vertical plate surrounded by a porous medium with large suction.

2. Mathematical Model of Flow

Consider a steady mixed convective heat transfer flow of an electrically conducting viscous fluid along an electrically non-conducting semi-infinite vertical plate embedded by a porous medium. The flow is also assumed to be in the *x*-direction which is taken along the plate in the upward direction and *y*-axis is normal to it. Initially, we consider that the plate as well as the fluid particles is at rest at the same temperature $T\left(=T_\infty\right)$ where T_∞ denotes the uniform temperature. It is assumed that the plate be at rest after that the plate is to be moving with a constant velocity U_0 in its own plane. It is also considered that the system is allowed to rotate with a constant angular velocity W about the *y*-axis. Hence the angular velocity vector is of the form $W = \left(0, -\Omega, 0\right)$.

In accordance with the usual Boussinesq's approximation, the equations relevant to the present problem are governed by the following system of coupled non-linear partial differential equations under the Ekman bounder layer Phenomena,

Continuity equation,

$$\frac{\partial u}{\partial x} + \frac{\partial v}{\partial y} = 0$$

Momentum equations,

$$u\frac{\partial u}{\partial x} + v\frac{\partial u}{\partial y} = g\,b\left(T - T_\infty\right) + u\frac{\partial^2 u}{\partial y^2} + 2\,\Omega w - \frac{u}{K}u$$

$$u\frac{\partial w}{\partial x} + v\frac{\partial w}{\partial y} = u\frac{\partial^2 w}{\partial y^2} - 2\,u\,\Omega - \frac{u}{K}w$$

Energy equation, $$u\frac{\partial T}{\partial x}+v\frac{\partial T}{\partial y}=\frac{k}{r\ c_p}\frac{\partial^2 T}{\partial y^2}+\frac{u}{c_p}\left[\left(\frac{\partial u}{\partial y}\right)^2+\left(\frac{\partial w}{\partial y}\right)^2\right]$$

with the appropriate boundary conditions,

$$u=U_0,\quad v=V(x),\quad w=0,\quad T=T_w\qquad \text{at } y\to 0$$
$$u=0,\quad v=0,\quad w=0,\quad T=T_\infty\qquad \text{as } y\to\infty$$

where y is the cartesian coordinate; u, v, w are velocity components; g is the local acceleration due to gravity, b is the thermal expansion coefficient, u is the kinematic viscosity, r is the density, k is the thermal conductivity and c_p is the specific heat at constant pressure.

3. Mathematical Formulation

In order to obtain the similar solutions of the mathematical model of flow, it is required to introduce the following similarity variables,

$$h=y\sqrt{\frac{U_0}{2\,u\,x}},\quad y=\sqrt{2uxU_0}\,f(h)\qquad \text{and}\qquad q(h)=\frac{T-T_\infty}{T_w-T_\infty}$$

Introducing the above stated variables, we have the followings,

$$u=U_0 f'(h),\quad v=\sqrt{\frac{u\ U_0}{2x}}\left[h f'(h)-f(h)\right]\qquad \text{and}\qquad w=U_0 g(h)$$

Using the above relations, we obtain the dimensionless equations,

$$f'''+ff''+G_r q-k f'+2Eg=0$$
$$g''+fg'-kg-2Ef'=0$$
$$q''+P_r fq'+P_r E_c\left(f''^2+g'^2\right)=0$$

where, $E=\frac{2\Omega x}{U_0}$ (**Ekman Number**), $P_r=\frac{r u c_p}{k}$ (**Prandtl Number**),

$G_r=\frac{2x}{U_0^2}gb\left(T_w-T_\infty\right)$ (**Grashof Number**), $E_c=\frac{U_0^2}{c_p\left(T_w-T_\infty\right)}$ (**Eckert Number**),

$K=\frac{2ux}{kU_0}$ (**Permeability Parameter**) and $f'(h)$, $g(h)$, $q(h)$ represent the non-dimensional primary velocity, secondary velocity and temperature respectively.

Also the boundary conditions are transformed to,

$$f=f_w,\quad f'=1,\quad g=0,\quad q=1\qquad \text{at}\quad h=0$$
$$f'=0,\quad g=0,\quad q=0\qquad \text{as}\quad h\to\infty$$

where, $f_w=-V(x)\sqrt{\frac{2x}{U_0 ?}}$ is the transpiration parameter. Here $f_w<0$ indicates the suction and $f_w>0$ denotes the injection.

4. Solution of the Problem

Since the solution is sought for the large suction, hence we make the following transformations,

$x = h f_w, \quad f(h) = f_w F(x), \quad g(h) = f_w^2 G(x)$ and $q(h) = f_w^2 H(x).$

Using the above quantities we have the following system of equations,

$$F''' + FF'' = e(k F' - G_r H - 2EG)$$

$$G'' + FG' = e(k G + 2EF')$$

$$H'' + P_r FH' + P_r E_c \frac{1}{e}\left(F''^2 + G'^2\right)$$

with the boundary conditions,

$$F = 1, \quad F' = e, \quad G = 0, \quad H = e \quad \text{at} \quad ? = 0$$

$$F' = 0, \quad G = 0, \quad H = 0 \quad \text{as} \quad ? \to \infty$$

where, $e = \frac{1}{f_w^2}$ is very small as for the large suction $(f_w > 1)$. Therefore we can expand F, G and H in terms of the small perturbation quantity e as follows,

$$F(x) = 1 + e F_1(x) + e^2 F_2(x) + e^3 F_3(x) + \ldots\ldots\ldots\ldots$$

$$G(x) = e\, G_1(x) + e^2 G_2(x) + e^3 G_3(x) + \ldots\ldots\ldots\ldots\ldots\ldots$$

$$H(x) = e\, H_1(x) + e^2 H_2(x) + e^3 H_3(x) + \ldots\ldots\ldots\ldots\ldots$$

Introducing $F(x)$, $G(x)$ and $H(x)$ in the above system of equations, we get the following first order equations,

$$F_1''' + F_1'' = 0$$

$$G_1'' + G_1' = 0$$

$$H_1'' + P_r H_1' + P_r E_c \left(F_1''^2 + G_1'^2\right) = 0$$

with the boundary conditions,

$$F_1 = 0, \quad F_1' = 1, \quad G_1 = 0, \quad H_1 = 1 \quad \text{at} \quad x = 0$$

$$F_1' = 0, \quad G_1 = 0, \quad H_1 = 0 \quad \text{at} \quad x \to \infty.$$

Also we obtain the second order equations,

$$F_2''' + F_2'' + F_1 F_1'' = kF_1' - G_r H_1 - 2EG_1$$

$$G_2'' + G_2' + F_1 G_1' = kG_1 + 2EF_1'$$

$$H_2'' + P_r\left(H_2' + F_1 H_1' + 2E_c F_1'' F_2'' + 2E_c G_1' G_2'\right) = 0$$

with the boundary conditions,

$$F_2 = 0, \quad F_2' = 0, \; G_2 = 0, \; H_2 = 0 \quad \text{at} \quad x = 0$$

$$F_2' = 0, \quad G_2 = 0, \quad H_2 = 0 \quad \text{at} \quad x \to \infty.$$

Using the prescribed boundary conditions, we have the first order solution,

$$F_1 = 1 - e^{-x}, \quad G_1 = 0, \quad H_1 = e^{-P_r x} + A_{11} e^{-2x}$$

as well as the second order solution of the system as follows,

$$F_2 = A_{20} ?e^{-x} + A_{21} e^{-P_r ?} + A_{22} e^{-2 ?}, \qquad G_2 = -2Ex\, e^{-x}$$

$$H_2 = A_{27} e^{-2x} - P_r x e^{-P_r x} + A_{28} e^{-x(P_r+1)} + A_{29} e^{-3x} + A_{30}(x + A_{31}) e^{-2x}$$

From the first and second order solution, the velocities and temperature fields are obtained as follows,

Primary velocity, $f'(h) = e^{-h f_w} + e\left(A_{20}e^{-h f_w} - A_{20} h f_w e^{-h f_w} - P_r A_{21} e^{-h f_w P_r} - 2A_{22} e^{-2h f_w}\right)$

Secondary velocity, $g(h) = -2U_0\, e\, E h f_w e^{-h f_w}$

Temperature, $q(h) = \left(e^{-h f_w P_r} + A_{11} e^{-2h f_w}\right)$

$$+e\left[A_{27}e^{-2h f_w} - h f_w P_r e^{-h f_w P_r} + A_{28} e^{-h f_w (P_r+1)} + A_{29} e^{-3h f_w} + A_{30}\left(h f_w + A_{31}\right) e^{-2h f_w}\right]$$

5. Shear Stress and Nusselt Number

Since the quantities of chief physical interest are shear stress and Nusselt number, hence the primary wall shear stress is defined as,

$$t_x = m\left(\frac{\partial u}{\partial y}\right)_{y=0}$$

which implies that, $t_x a \left[-1 + e\left(-2A_{20} + P_r^2 A_{21} + 4A_{22}\right)\right]$.

The secondary wall shear stress is also defined as,

$$t_z = \mu\left(\frac{\partial w}{\partial y}\right)_{y=0}$$

which implies that, $t_z a \left(-2eE\right)$.

As well as the Nusselt number is defined as,

$$N_u = \mu\left(-\frac{\partial T}{\partial y}\right)_{y=0}$$

which implies that, $N_u a \left[\left(-P_r - 2A_{11}\right) + e\left[-2A_{27} - P_r - A_{28}\left(P_r + 1\right) - 3A_{29} + A_{30} - 2A_{30}A_{31}\right]\right]$.

6. Results and Discussion

In order to discuss the results of the present work, the analytical solutions are obtained by perturbation technique. For investigating the physical situation of the model, we have computed the numerical values of the flow variables(velocities and temperature) for different values of suction parameter, Grashof number, Prandtl number, Eckert number, Ekman number as well as permeability parameter. In this section, the numerical values of the velocities and fluid temperature versus h are plotted in Figures 6.1-6.8.

The primary velocity profiles for different values of G_r, K, P_r and E_c are shown in Figures 6.1-6.4. From Figure 6.1, we see that the primary velocity increases with the increase of G_r. It is observed from Figure 6.2 that the primary velocity decreases with the rise of K and the same effect of the Prandtl number on the primary velocity is observed from Figure 6.3. An increasing effect on the primary velocity profiles for E_c is found from the Figure 6.4.

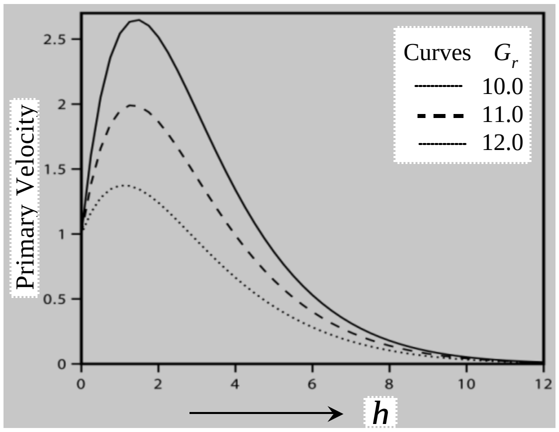

Figure 6.1. Primary Velocity Profiles for $f_w = 2.0,\ K = 0.1,\ E = 1.0,\ P_r = 7.0,\ E_c = 1.0$.

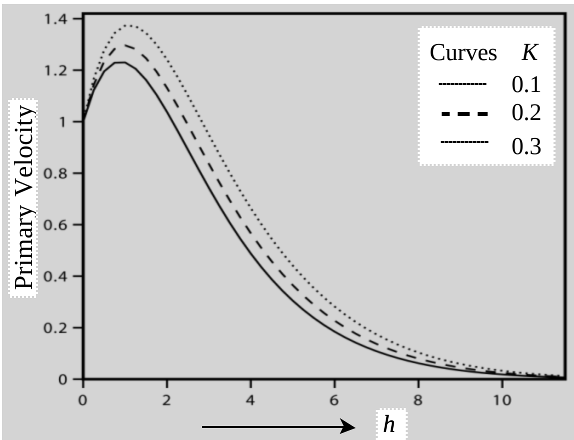

Figure 6.2. Primary Velocity Profiles for $G_r = 10,\ f_w = 2.0,\ E = 1.0,\ P_r = 7.0,\ E_c = 1.0$.

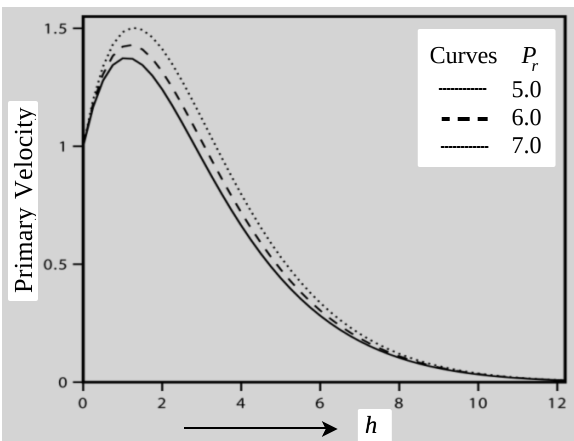

Figure 6.3. Primary Velocity Profiles for $G_r = 10,\ f_w = 2.0,\ K = 0.1,\ E = 1.0,\ E_c = 1.0$.

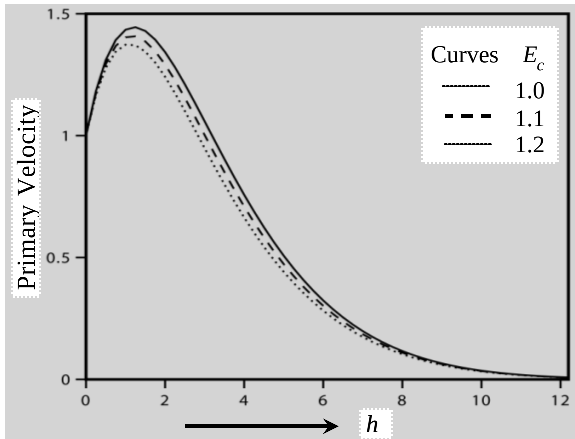

Figure 6.4. Primary Velocity Profiles for $G_r = 10$, $f_w = 2.0$, $K = 0.1$, $E = 1.0$, $P_r = 7.0$.

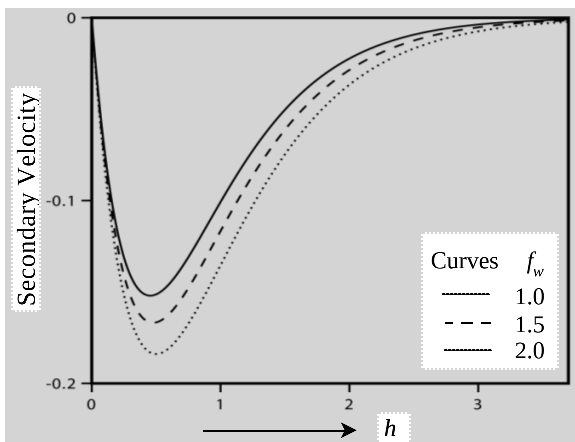

Figure 6.5. Secondary Velocity Profiles for $G_r = 10$, $K = 0.1$, $E = 1.0$, $P_r = 7$, $E_c = 1.0$.

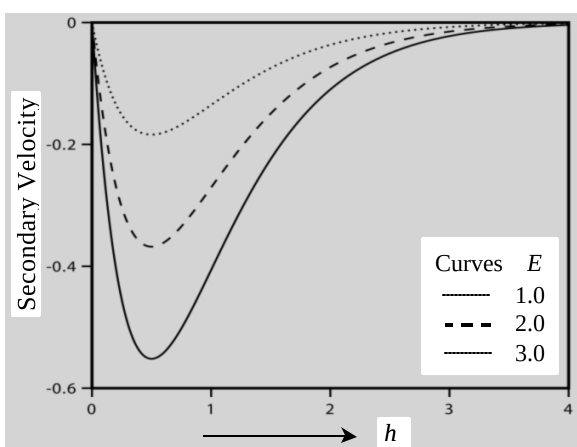

Figure 6.6. Secondary Velocity Profiles for $G_r = 10$, $f_w = 2$, $K = 0.1$, $P_r = 7$, $E_c = 1.0$.

The secondary velocity curves for different values of f_w and E are displayed in Figures 6.5-6.6. It is observed from the Figure 6.5, the secondary velocity decreases with the increase of the Ekman Number. The Figure 6.6 shows that the secondary velocity increases with the rise of f_w.

The temperature distributions of fluid are shown in Figures 6.7-6.8. From the two figures, we have observed the temperature decreases with the increases of E_c as well as the temperature rises in case of strong Prantdl number.

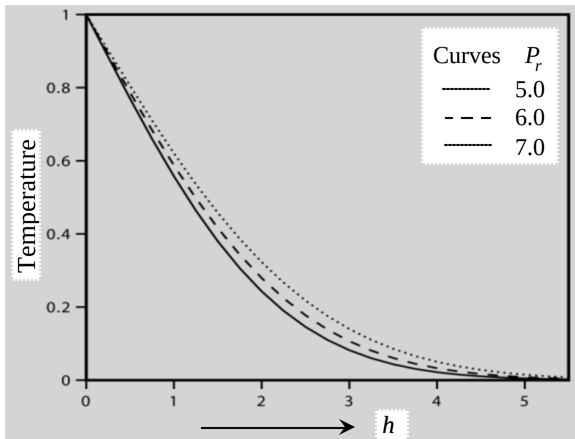

Figure 6.7. Temperature Profiles for $G_r = 10$, $f_w = 2.0$, $K = 0.1$, $E = 1.0$, $E_c = 1.0$.

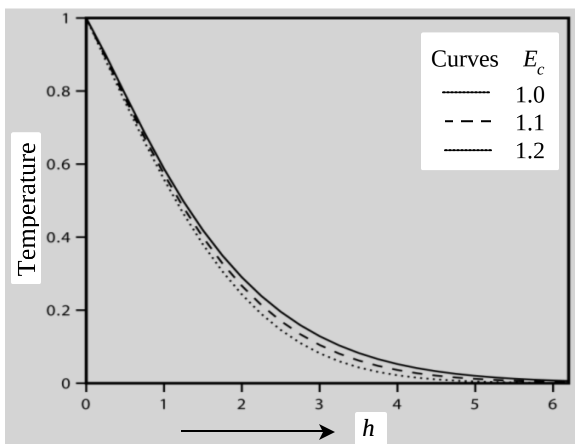

Figure 6.8. Temperature Profiles for $G_r = 10$, $f_w = 2.0$, $K = 0.1$, $E = 1.0$, $P_r = 7.0$.

To discus the quantities of chief physical interest of the problem, the numerical values of primary shear stress (t_x), secondary shear stress (t_z) and Nusselt number (N_u) are tabulated in the following Table 6.1 due to the variation in G_r, f_w, K, E, P_r and E_c for an externally cooled $(G_r > 0)$ plate.

It is observed from Table 6.1, the primary shear stress at the wall increases in case of strong of G_r or E_c while it decreases with the rise of P_r, f_w or K but it remains unchanged with the change of E. We see that, the secondary shear stress at the wall increases for rising the f_w while it decreases with the increase of E but no effect is found by the change of G_r, P_r, K or E_c. Also the Nusselt number increases in case of strong G_r, f_w, K or E_c while it decreases the rise of Prandtl number but it remains unchanged with the change of Ekman number.

Table 6.1. Numerical Values of Shear Stresses $(t_x \& t_z)$ with Nusselt Number

S. No.	G_r	f_w	K	E	P_r	E_c	t_x	t_z	N_u
1.	10.0	2.0	0.1	1.0	7.0	1.0	**0.217**	**-0.500**	**3.871**
2.	11.0	2.0	0.1	1.0	7.0	1.0	**0.271**	**-0.500**	**4.367**
3.	12.0	2.0	0.1	1.0	7.0	1.0	**0.325**	**-0.500**	**4.863**
4.	10.0	2.1	0.1	1.0	7.0	1.0	**0.157**	**-0.454**	**4.292**
5.	10.0	2.2	0.1	1.0	7.0	1.0	**0.112**	**-0.413**	**4.657**
7.	10.0	2.0	0.2	1.0	7.0	1.0	**0.204**	**-0.500**	**4.011**
8.	10.0	2.0	0.3	1.0	7.0	1.0	**0.192**	**-0.500**	**4.151**
9.	10.0	2.0	0.1	2.0	7.0	1.0	**0.217**	**-1.000**	**3.871**
10.	10.0	2.0	0.1	3.0	7.0	1.0	**0.217**	**-1.500**	**3.871**
11.	10.0	2.0	0.1	1.0	5.0	1.0	**0.352**	**-0.500**	**6.931**
12.	10.0	2.0	0.1	1.0	6.0	1.0	**0.269**	**-0.500**	**5.796**
13.	10.0	2.0	0.1	1.0	7.0	1.1	**0.260**	**-0.500**	**4.512**
14.	10.0	2.0	0.1	1.0	7.0	1.2	**0.304**	**-0.500**	**5.135**

7. Conclusions

Some of the important findings obtained from the graphical representation of the results with the numerical values of table are listed below;

1. The primary fluid velocity increases with the increase of G_r or E_c while it decreases with the increase of P_r or K.
2. The secondary velocity of fluid increases with the increase of f_w while it decreases with the increase of E.
3. The fluid temperature is increasingly affected by P_r and decreasingly affected by E_c.
4. The primary shear stress at the wall increases in case of strong G_r or E_c while decreases with the increase of P_r, f_w or K.
5. The secondary shear stress at the wall increases in case of strong f_w while decreases with the increase of E.
6. The Nusselt number increases with the increase of G_r, f_w, K or E_c while it decreases in case of strong Prandtl number.

Appendix

$$A_{11} = \frac{E_C \quad P_r}{2\ P_r\text{-}4}, \quad A_{20} = 1 + k, \quad A_{21} = \frac{G_r}{P_r^{\,2}\,(P_r - 1)}, \quad A_{22} = \left(\frac{1 + G_r A_{11}}{4}\right),$$

$$A_{23} = P_r\,(2A_{11} - 4A_{20}E_c),\ A_{24} = P_r^{\,2}\,(2P_r E_c A_{21} - 1),\ A_{25} = P_r\,(8A_{22}E_c - 2A_{11}),\ A_{26} = 2A_{20}P_r E_c\,,$$

$$A_{27} = \frac{A_{23}}{(4 - 2P_r)}, \quad A_{28} = \frac{A_{24}}{1 + P_r}, \quad A_{29} = \frac{A_{25}}{(9 - 3P_r)}, \quad A_{30} = \frac{A_{26}}{4 - 2P_r} \text{ and } A_{31} = \frac{4 - P_r}{4 - 2P_r}.$$

REFERENCES

1. A. Raptis, G. Tzivanidis and N. Kafousias, Free convection and mass transfer flow through a porous medium bounded by an infinite vertical limiting surface with constant suction, *Letters Heat and Mass Transfer*, 8(5) (1981), 417-424.
2. K. Yamamoto and N. Iwamura, Flow with convective acceleration through a porous medium, *J. Engi. Math.*, 10(1) (1976) 41-54.
3. R.C. Chaudhury and T. Chand, Three dimensional flow and heat transfer through a porous medium, *Int. J. Appl. Mech. Engi.*, 7(4) (2002), 1141-1156.
4. H.P. Greenspan, *The Theory of Rotating Fluids*, Cambridge University Press, Cambridge, 1968.
5. G.K. Batchelor, *An Introduction to Fluid Dynamics*, Cambridge University Press, Cambridge, 1970.
6. B.S. Mazumder, A.S. Gupta and N. Datta, Flow and heat transfer in the hydromagnetic ekman layer on a porous plate with hall effects, *Int. Journal of Heat and Mass Transfer*, 19(5) (1976) 523-527.
7. A.K. Singh, Hydromagnetic free convection flow past an impulsively started vertical plate in a rotating system, *Int. Com. Heat Mass Transfer*, 11 (1984), 349.